

Multi-Period Sparse Optimization for Proactive Grid Blackout Diagnosis

Qinghua Ma¹, Reetam Sen Biswas², Denis Osipov³, Guannan Qu⁴, Soummya Kar⁴, Shimiao Li¹

¹EE Dept., University at Buffalo {qinghuam, shimiaol}@buffalo.edu

²GE Vernova Advanced Research {Reetam.SenBiswas}@gevernova.com

³New York Power Authority {denis.osipov}@nypa.gov

⁴ECE Dept., Carnegie Mellon University {gqu, soummyak}@andrew.cmu.edu

Abstract—Existing or planned power grids need to evaluate survivability under extreme events, like a number of peak load overloading conditions, which could possibly cause system collapses (i.e. blackouts). For realistic extreme events that are correlated or share similar patterns, it is reasonable to expect that the dominant vulnerability or failure sources behind them share the same locations but with different severity. Early warning diagnosis that proactively identifies the key vulnerabilities responsible for a number of system collapses of interest can significantly enhance resilience. This paper proposes a multi-period sparse optimization method, enabling the discovery of persistent failure sources across a sequence of collapsed systems with increasing system stress, such as rising demand or worsening contingencies. This work defines persistency and efficiently integrates persistency constraints to capture the “hidden” evolving vulnerabilities. Circuit-theory based power flow formulations and circuit-inspired optimization heuristics are used to facilitate the scalability of the method. Experiments on benchmark systems show that the method reliably tracks persistent vulnerability locations under increasing load stress, and solves with scalability to large systems (on average taking around 200 s per scenario on 2000+ bus systems).

Index Terms—blackout diagnosis, multi-period optimization, power system resiliency, sparse optimization, vulnerability analysis

I. INTRODUCTION

The power grid is increasingly challenged by extreme events (such as extreme heat or cold) and cyber threats [1], lacking resilience to which can result in system collapses (i.e., blackouts). In June 2025, a severe heatwave pushed New York’s electric grid to its limits, triggering widespread outages across the Tri-State area affecting thousands of Queens residents. The 2021 Texas power crisis [2], caused by extreme cold in winter, left 4.5 million homes without power. Ukraine Cyber-attacks in 2015-2016 [3][4] brought down sections of the Ukrainian power grid causing power outages for roughly 230,000 consumers. New attack models such as MadIoT [5][6] are theoretically capable of manipulating load demand at a large number of locations to make the system unstable or collapse.

Manuscript submitted to PSCC 2026.

With the growing threats, power system operators and planners increasingly need to evaluate survivability under a large set of extreme events (e.g. a set of possible peak or abnormal load conditions) which could possibly cause system collapse [7]. Early diagnosis that proactively detects the vulnerability of the system and identifies the impact of the failure can significantly enhance reliability and resiliency against high-impact failures.

Today’s grid operators and planners mainly perform such routine evaluations using the industry-standard power flow simulators [8] that find a feasible solution from steady-state power flow equations. As a collapsed system mathematically represents an infeasible system whose solution does not exist, these steady-state simulators will diverge and thus return limited information. Later works [9][10][11] introduce slack variables to capture the violation of system feasibility constraints and thus are able to converge with the severity of collapse quantified. More recently, our prior work [12] proposed a sparse optimization framework that rapidly identifies a minimal set of critical locations responsible for a given system collapse, offering targeted insights into the dominant sources of failure and locating key system vulnerabilities. Later works have extended this to distribution systems [13], as well as combined transmission and distribution networks [14].

However, these advancements are designed to evaluate a single scenario case, and fail to consider multiple important scenarios together which are likely during extreme event situations. In reality, operators and planners are concerned with many extreme situations that a power grid may face, e.g., a series of anticipated load growth over the next 10 years. Since these multiple scenarios are strongly correlated, sorting them in the order of growing stress naturally forms a practical multi-period sequential problem. Note that the term ‘multi-period’ in this work does not refer to fixed time steps, but a sequence of events that are correlated by stress levels. In this setting, it is both intuitive and reasonable to expect that a few key vulnerability locations persist across multiple scenarios, with their severity gradually increasing. By identifying and addressing these hidden “persistent” vulnerabilities, decision-makers can desirably reduce blackout risks in an effective and targeted way.

This paper extends the state-of-the-art single-scenario works

to multi-period sparse diagnosis, enabling the discovery of persistent failure sources over a sequence of collapsed scenarios triggered by increasing stress, such as rising demand or worsening contingencies. Unlike independently analyzing each single scenario, this paper defines “persistency” and formulates a novel *sparse optimization with persistency prior*. In this way, we integrate temporal persistency constraints on failure source locations to capture the evolving system vulnerabilities hidden behind blackouts. To solve the problem at scale for large systems, we leverage the efficient location-wise sparse optimization technique [12] and propose to enforce persistency using a soft constraint on sparsity coefficients. We also formulate system constraints under circuit-theory based formulations and adopt circuit-inspired optimization heuristics [10] to facilitate scalability to large systems.

Our results in Figure 1 show that the method reliably tracks persistent failure locations under increasing load demand stress, and solves with scalability to large systems (2383 buses in Figure 1(b)). These capabilities support focused decision-making to identify and further reduce blackout risk in both operations and planning, enhancing blackout resilience.

Findings of this work will also boost planning efficiency through immediate projections. With the underlying vulner-

abilities captured with temporal correlations, solutions from selected load-growth scenarios can be interpolated to intermediate cases. For example, in Figure 1a, node 19 in the 30-bus system is dominant in load factors 3.8 and 3.9, then it can be expected to remain vulnerable for intermediate load factors such as 3.86 even without explicitly solving. In practice, since it is computationally prohibitive to evaluate every critical case, such projections enable efficient assessment across a wide stress range.

II. RELATED WORK

A. Regular power flow analysis for collapsed systems

As mentioned earlier, the traditional steady-state power flow analysis converges to a feasible solution v^* by solving the nonlinear AC power flow equations $g(v) = 0$ that characterize network balance under either polar coordinate (where state v_i at each bus i represents voltage magnitude $|V_i|$ and phase angle θ_i) or rectangular coordinate (where state v_i at bus i represents real and imaginary voltage $V_i^{\text{Real}}, V_i^{\text{Imag}}$); however, if no feasible solution exists for the network, the solver diverges, resulting in limited information. To avoid such divergence, approaches [9][11] to capture and quantify infeasibility within power flow analysis were developed to quantify the potential

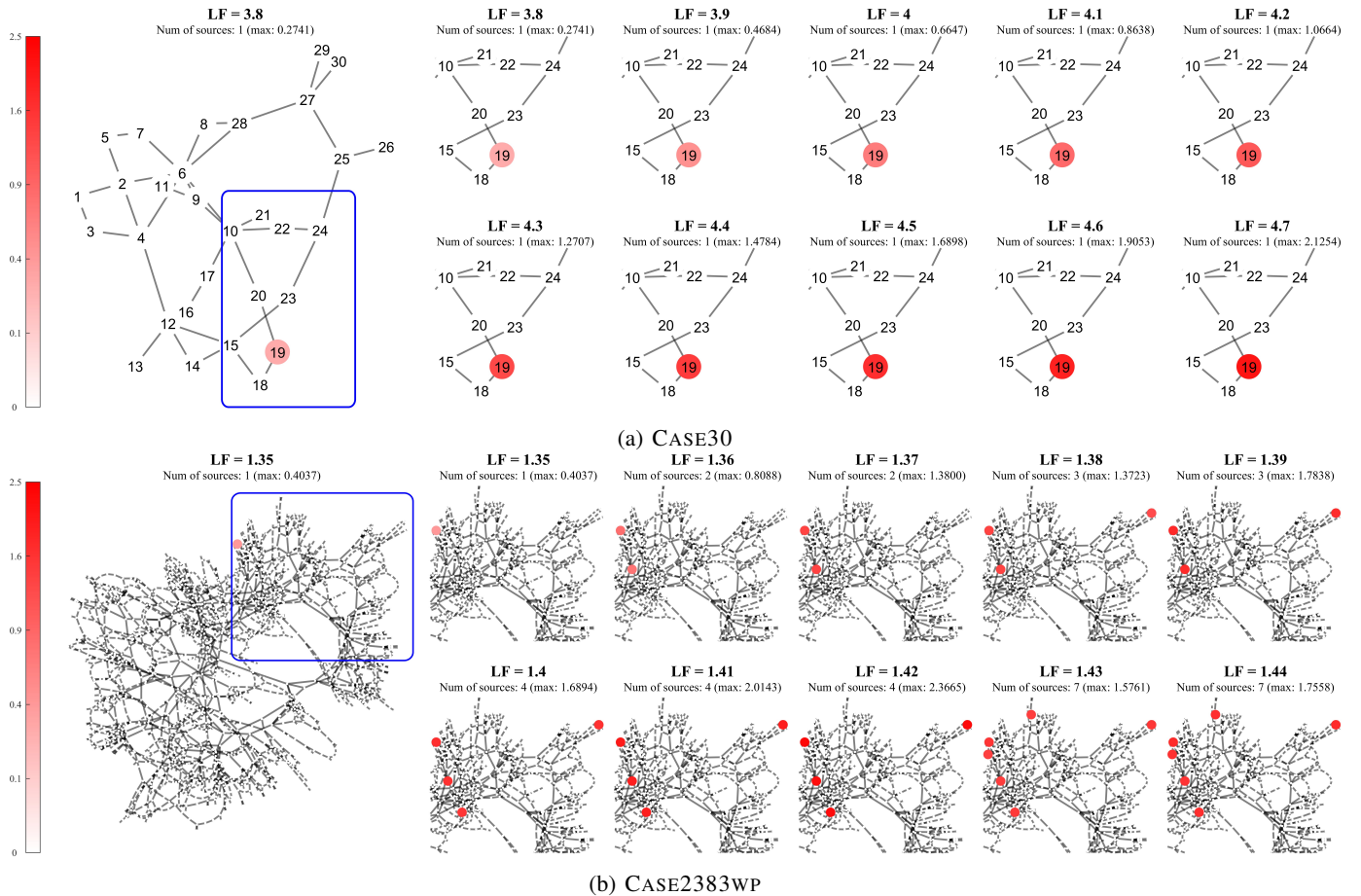


Fig. 1: With the growing demand stress, the proposed method identifies a gradually expanding set of system vulnerabilities with severity quantified.

infeasibility within the grid. The approach in [9] introduces slack variable $\mathbf{n}_i = \mathbf{n}_i^{Real} + \mathbf{n}_i^{Imag}$ to represent “infeasibility” at each bus i . These values represent compensation terms that capture how much additional resource is needed at each bus to make the network balance conditions hold. This infeasibility-quantified power flow study is formulated as a non-convex optimization problem:

Problem 1 (Dense optimization)

$$\min_{\mathbf{v}, \mathbf{n}} \frac{1}{2} \|\mathbf{n}\|_2^2, \text{ s.t. } g_i(\mathbf{v}) + \mathbf{n}_i = 0, \forall i \quad (1)$$

This formulation can clearly identify a collapsed system (infeasible) from a feasible one. Besides, convergence with nonzero \mathbf{n} vector denotes an infeasible system with severity of power flow deficiency quantified by the magnitude of \mathbf{n} .

B. Sparse diagnosis for collapsed systems

Although advanced power flow studies [9][11] above can converge for a collapsed grid, they do not indicate specific cause of collapse, nor do they detect locations that are disrupting power system security and robustness. In most situations, it would be desirable to know the smallest possible set of dominant nodes that are causing system collapse with some quantifiable metric. Accurate and efficient localization of this dominant set of nodes identifies the deficiency of power (real and reactive) and highlights some critical locations for special attention in the planning process. For instance, consider reactive power planning (RPP) problems [15][16][17][18] that aim to find the optimal allocation of reactive power support through capacitor banks or FACTS devices such as static VAR compensators (SVC). Such problems correspond to finding the sparsest reactive power compensation vector that satisfies system power balance and operation limits in an optimization-based power flow study. However, solving such optimization problems at scale is challenging. Location selection is typically treated by introducing binary variables, leading to the formulation of mixed-integer programming (MIPs) that suffers from combinatorial complexity. Numerous nonlinear equality and inequality constraints further enlarge the problem size and increase non-convexity.

To efficiently locate system vulnerabilities and facilitate efficient proactive defense against system collapses, [12] introduced an efficient sparse optimization method. The objective of this method is to provide the minimal set of (sparse) locations, along with quantified slack sources that can be added to these locations, to restore system feasibility:

Given a (single) case scenario $\mathbf{g}(\mathbf{v})$, if system is collapsed (i.e., infeasible), find a sparse \mathbf{n} vector that restores feasibility; and return the set of locations $\{i \mid |n_i| > \varepsilon\}$ recognized as dominant sources of system failure or vulnerability ($\varepsilon = 10^{-6}$ in this work).

Problem 2 (Sparse Optimization)

$$\min_{\mathbf{x}, \mathbf{n}} \frac{1}{2} \|\mathbf{n}\|_2^2 + \sum_i c_i |\mathbf{n}_i|, \text{ s.t. } g_i(\mathbf{v}) + \mathbf{n}_i = 0, \forall i \quad (2)$$

Unlike the formulation in (1) above that minimizes the sum of squares (L2-norm) and leads to slack sources appearing everywhere in the solution, the proposed approach (2) localizes non-zero n_i sources at sparse locations using a novel variant of L1-regularization technique. To efficiently enforce sparsity, the method assigns location-wise sparsity coefficient c_i to each location i and adaptively toggles them to reach highly sparse solutions without requiring large coefficient values, thus removing the risk of ill-conditioning and facilitating efficient convergence. [12] demonstrated the efficacy of the sparse diagnosis approach in large systems up to the size of Eastern Interconnection network ($>80,000$ buses) and recognized 1 dominant failure source (vulnerability) when load demand increased by 7%.

C. Circuit-theoretic modeling of power grid

A circuit-theoretic formulation for power flow and grid optimizations, leveraging the heuristics developed in the field of circuit simulation [19] to efficiently solve large scale power system problems. Instead of defining state variables (voltage magnitude $|V|$ and phase angle δ) under polar coordinate and writing power balance equations, this framework models each component within the power grid as an equivalent circuit characterized by its current-voltage ($I - V$) relationship under rectangular coordinate. The $I - V$ relationships can represent both transmission and distribution grids without loss of generality and existing works have seen its application to power flow analysis [9][10], state estimation [20][21][22][23], optimal power flow analysis [24], etc. Under circuit-theoretic modeling, power system’s network constraints are characterized by Kirchhoff’s Current Law (KCL) equations. For computational analyticity, the complex functions are split into real and imaginary sub-circuits whose nodes correspond to power system buses.

This equivalent circuit formulation enables power systems of any size to be efficiently simulated as an equivalent circuit, numerous convergence techniques that were developed for circuit simulation (e.g. SPICE [19]) can be applied [10].

III. MULTI-PERIOD SPARSE DIAGNOSIS

Task Goal: Given a set of scenarios $\{1, 2, \dots, T\}$ sorted in the order of growing stress to form a multi-period setting, our goal is to find the sparsest and optimal $\mathbf{n}^{(1)}, \mathbf{n}^{(2)}, \dots, \mathbf{n}^{(T)}$ vectors that can restore feasibility; and meanwhile recognize dominant vulnerability (or failure source) location sets $\mathcal{S}^{(1)}, \mathcal{S}^{(2)}, \dots, \mathcal{S}^{(T)}$ with desired *persistency*. Here, the **vulnerability location set** $\mathcal{S}^{(t)} = \{i \mid |n_i^{(t)}| > \varepsilon\}$ is defined as the minimal set of locations whose compensations can restore feasibility for scenario t ($\varepsilon = 10^{-6}$).

The ideal persistency to be encouraged in our optimal solution is defined below:

Definition 1 (Ideal persistency of vulnerability locations)

Let us define vulnerability location set $\mathcal{S}^{(t)}$ as the minimal set of locations whose compensations can restore feasibility for scenario t . Under a multi-period setting $t = 1, 2, \dots, T$

with growing stress, the vulnerability location trajectory with ideal persistency satisfies:

$$\mathcal{S}^{(1)} \subseteq \mathcal{S}^{(2)} \subseteq \dots \subseteq \mathcal{S}^{(T)} \quad (3)$$

Equivalently, a vulnerability location i with ideal persistency satisfies:

$$\text{if } i \in \mathcal{S}^{(t)} \implies i \in \mathcal{S}^{(t+1)}, \forall t \leq T-1$$

or, in terms of the sparse indicator,

$$\text{if } |n_i^{(t)}| > \varepsilon \implies |n_i^{(t+1)}| > \varepsilon, \forall t \leq T-1$$

This intuitively means that once a location shows up as vulnerable, it stays vulnerable in all subsequent scenarios, revealing a critical weakness of the system as the stress keeps increasing.

However, when analyzing multiple scenarios in practice, the solution may not always satisfy ideal persistency, motivating us to define metrics to quantify the level of persistency achieved. We first define the location persistency metric for each vulnerability source location:

Definition 2 (Location Persistency Metric)

For a location i under a multi-period setting $t = 1, 2, \dots, T$, let k denote the first scenario index at which i becomes a vulnerability location, i.e., $k = \min\{t \mid i \in \mathcal{S}^{(t)}, t \leq T-1\}$. Firstly, if no such k exists, we set $\text{Persistency}(i) = 0$, representing that location i is never a vulnerable location. Secondly, if location i fails to remain vulnerable for at least 2 consecutive steps, we also set $\text{Persistency}(i) = 0$, representing that vulnerability at i occasionally occurs but never persists. In all remaining cases, we define the *persistency* of i as the proportion of subsequent time steps in which i continues to be vulnerable after it first showed up

$$\text{Persistency}(i) = \frac{\sum_{t=k}^T \mathbf{1}_{\{i \in \mathcal{S}^{(t)}\}}}{T - k + 1} \times 100\% \quad (4)$$

where $\mathbf{1}_{\{\cdot\}}$ is the indicator function, equal to 1 if the condition $\{\cdot\}$ is satisfied and 0 otherwise. This metric satisfies:

- 1) $0 \leq \text{Persistency}(i) \leq 100\%, \forall i$.
- 2) $\text{Persistency}(i) = 100\%$ if and only if i has ideal persistency, i.e., it remains vulnerable at all scenarios $k+1, \dots, T$ after first showing up at step k .

In addition to location persistency, we also quantify the overall network-level persistency of all vulnerability locations, by defining set persistency as below:

Definition 3 (Set Persistency Metric)

From scenario 1 to any scenario t , we are able to quantify how well the ideal persistency $\mathcal{S}^{(1)} \subseteq \mathcal{S}^{(2)} \subseteq \dots \subseteq \mathcal{S}^{(t-1)} \subseteq \mathcal{S}^{(t)}$ has been enforced so far, by:

$$\text{SetPersistency}(t) = \frac{|\mathcal{S}^{(t)}|}{|\cup_{j=1}^t \mathcal{S}^{(j)}|} \times 100\% \quad (5)$$

where $|\mathcal{S}|$ denotes set cardinality, i.e., the number of elements in set S ; and $\cup_{j=1}^t \mathcal{S}^{(j)} = \mathcal{S}^{(1)} \cup \mathcal{S}^{(2)} \cup \dots \cup \mathcal{S}^{(t-1)} \cup \mathcal{S}^{(t)}$ denotes the union of all vulnerability sets so far, which corresponds to a set of all vulnerability locations identified across $1, 2, \dots, t$. This metric satisfies:

- $0 \leq \text{SetPersistency}(t) \leq 100\%, \forall t$.
- When ideal persistency holds, we will have $\mathcal{S}^{(t)} = \cup_{j=1}^t \mathcal{S}^{(j)}$, so that $\text{SetPersistency}(t) = 100\%$.

A. Method overview

With the task goal and preliminaries defined above, this paper will model the inter-dependence across the multiple scenarios analyzed.

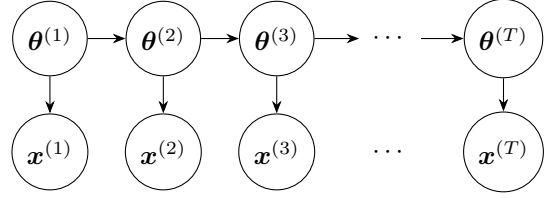


Fig. 2: Bayesian Network illustration of multi-period model

For any scenario t , let the hidden variable $\boldsymbol{\theta}^{(t)} = [\theta_1^{(t)}, \dots, \theta_i^{(t)}, \dots, \theta_N^{(t)}]$ be a vector of status variables representing whether each bus location $i \in \{1, 2, \dots, N\}$ is a vulnerability source, i.e. $\theta_i^{(t)} = 1$ if $i \in \mathcal{S}^{(t)}$ or equivalently if $|n_i^{(t)}| > \varepsilon$.

Instead of treating each scenario independently, we adopt a Bayesian Network in Figure 2 as a conceptual lens to capture how hidden vulnerabilities evolve across stress levels, with the sparse optimization output of each scenario serving as a “noisy observation” of these hidden vulnerabilities. Specifically, the system starts with an initial hidden vulnerability $\boldsymbol{\theta}^{(1)}$. At any time t , the change in system stress drives the vulnerability to change incrementally from $\boldsymbol{\theta}^{(t-1)}$ to $\boldsymbol{\theta}^{(t)}$. And each vulnerability stage $\boldsymbol{\theta}^{(t)}$ leads to its corresponding state variables $\mathbf{x}^{(t)} = [n^{(t)}, v^{(t)}]$ that include the targeted compensations $n^{(t)}$ needed to restore its feasibility and the voltages $v^{(t)}$ of the feasible “reconstructed” system. The sparse diagnosis method can be considered a sensor or lens from which we can obtain \mathbf{x} as an “tentative observation” of hidden variables $\boldsymbol{\theta}$ and thus locate the hidden vulnerabilities accordingly.

Under this view, vulnerabilities $\boldsymbol{\theta}^{(1)}, \dots, \boldsymbol{\theta}^{(t)}$ and outputs $\mathbf{x}^{(1)}, \dots, \mathbf{x}^{(t)}$ across all scenarios can be considered jointly, and the Bayesian factorization highlights that the key components are the transition probabilities $P(\boldsymbol{\theta}^{(j)} | \boldsymbol{\theta}^{(j-1)})$ and the likelihood terms $P(\mathbf{x}^{(j)} | \boldsymbol{\theta}^{(j)})$:

$$\begin{aligned} & \boldsymbol{\theta}^{(1)*}, \dots, \boldsymbol{\theta}^{(t)*}, \mathbf{x}^{(1)*}, \dots, \mathbf{x}^{(t)*} \\ &= \arg \max P(\boldsymbol{\theta}^{(1)}, \dots, \boldsymbol{\theta}^{(t)}, \mathbf{x}^{(1)}, \dots, \mathbf{x}^{(t)}) \\ &= \arg \max P(\boldsymbol{\theta}^{(1)}) P(\mathbf{x}^{(1)} | \boldsymbol{\theta}^{(1)}) \cdot \prod_{j=2}^t P(\boldsymbol{\theta}^{(j)} | \boldsymbol{\theta}^{(j-1)}) P(\mathbf{x}^{(j)} | \boldsymbol{\theta}^{(j)}) \end{aligned} \quad (6)$$

Considering a multi-period processing in the forward direction, the task above can be split into 2 subtasks:

- 1) sparse optimization with persistency prior: For each scenario t ($t \geq 2$), given $\theta^{(t-1)}$ from previous stage, the problem reduces to a single-scenario optimization augmented by the prior probability $P(\theta^{(t)}|\theta^{(t-1)})$:

$$\begin{aligned} & \theta^{(t)*}, \mathbf{v}^{(t)*}, \mathbf{n}^{(t)*} \\ &= \arg \max P(\theta^{(t)}|\theta^{(t-1)})P(\mathbf{v}^{(t)}, \mathbf{n}^{(t)}|\theta^{(t)}) \end{aligned} \quad (7)$$

- 2) getting the prior distribution $P(\theta^{(1)})$ for $t = 1$, so that $\theta^{(1)*}, \mathbf{v}^{(1)*}, \mathbf{n}^{(1)*}$ can be optimized similarly as above.

In practice, however, the exact distribution functions are only partially tractable or entirely intractable (although they theoretically exist), so exact inference from the full joint distribution is impractical. Therefore, the remainder of this section develops sparse optimization as a deterministic relaxation of the Bayesian inference problem, while still embedding the notion of vulnerability evolution into our optimization framework.

B. Sparse optimization with persistency prior

Without prior information on $\theta^{(t)}$ for scenario t , one may consider every location has the same probability of being a dominant vulnerability source; in which case solving the single-scenario sparse optimization in Problem 2 can be seen as finding the most possible $\theta^{(t)*}, \mathbf{v}^{(t)*}, \mathbf{n}^{(t)*} = \arg \max P(\theta^{(t)})P(\mathbf{v}^{(t)}, \mathbf{n}^{(t)}|\theta^{(t)})$ with prior Bernoulli distribution $P(\theta_i^{(t)} = 1) = p$ for $\forall i$, where p is a constant.

Now, given prior knowledge $\theta^{(t-1)}$ from the previous stage $t-1$, we can model and integrate a more informative prior distribution $P(\theta^{(t)}|\theta^{(t-1)})$ to encourage the ideal persistency on stage t , which, based on our definition, can be illustrated as a state transition probability $P(\theta_i^{(t)} = 1|\theta_i^{(t-1)} = 1) = 100\%$. This equivalently represents some additional hard constraints on the binary status variables $\theta_i^{(t)}$ so that the problem $\theta^{(t)*}, \mathbf{v}^{(t)*}, \mathbf{n}^{(t)*} = \arg \max P(\theta^{(t)}|\theta^{(t-1)})P(\mathbf{v}^{(t)}, \mathbf{n}^{(t)}|\theta^{(t)})$ becomes:

$$\begin{aligned} & \min_{\mathbf{v}, \mathbf{n}} \frac{1}{2} \|\mathbf{n}\|_2^2 + \sum_i c_i |\mathbf{n}_i| \\ & \text{s.t. } g_i(\mathbf{v}) + \mathbf{n}_i = 0, \forall i \\ & \text{additional constraint (a): } \theta_i^{(t)} = \mathbf{1}_{\{|\mathbf{n}_i^{(t)}| > \epsilon\}}, \forall i \\ & \text{additional constraint (b): } \theta_i^{(t)} \geq \theta_i^{(t-1)}, \forall i \end{aligned} \quad (8)$$

where the additional constraint (a) defines the binary status variable, and (b) enforces the ideal persistency (for each location).

The above problem is mathematically a mixed-integer programming, which can be hard to solve due to its combinatorial nature. If solution at $t-1$ is available, one might attempt to remove the mixed-integer variables by equivalently transforming constraints (a) and (b) into $|\mathbf{n}_i^{(t)}| \geq \epsilon$, for $\forall i \in \mathcal{S}^{(t-1)}$, which is a nonlinear and nonconvex hard constraint since $|\mathbf{n}_i^{(t)}| = |\mathbf{n}_i^{(t)Real} + j \cdot \mathbf{n}_i^{(t)Imag}| = \sqrt{(\mathbf{n}_i^{(t)Real})^2 + \mathbf{n}_i^{(t)Imag})^2}$.

However, practical optimization heuristics that can efficiently enforce sparsity-inducing hard constraints are not readily available. Moreover, ideal persistency may not always be achievable in realistic systems, and enforcing constraint (b) rigidly can lead to no solution or suboptimal solutions with sparsity degraded.

To more efficiently solve the multi-period sparse optimization, we propose to transform the above problem into an equivalent form where we get rid of mixed integers and encourage ideal persistency as a soft constraint. The new problem is defined below:

Problem 3 (Sparse Optimization with persistency prior)

$$\begin{aligned} & \min_{\mathbf{v}, \mathbf{n}} \frac{1}{2} \|\mathbf{n}\|_2^2 + \sum_i c_i^{(t)} |\mathbf{n}_i| \\ & \text{s.t. } g_i(\mathbf{v}) + \mathbf{n}_i = 0, \forall i \\ & \text{sparsity coefficients: } c_i^{(t)} \leq c_i^{(t-1)}, \forall i \end{aligned} \quad (9)$$

where we embed ideal persistency into the tuning of sparsity coefficients in each scenario.

Leveraging the efficient location-wise sparsity enforcement mechanism proposed in [12], where the sparsity coefficients $c_i^{(t)}$ are iteratively and adaptively switched between $c_H = 10$ and $c_L = 0.1$ to promote sparse solutions $\mathbf{n}^{(t)}$ for each scenario t . At each update, locations with high $\mathbf{n}_i^{(t)}$ values are assigned with c_L ; whereas those with lower $\mathbf{n}_i^{(t)}$ are assigned with c_H . Upon convergence, $c_i^{(t)} = c_H$ promotes zero $|\mathbf{n}_i^{(t)}|$ and $c_i^{(t)} = c_L$ promotes non-zero $|\mathbf{n}_i^{(t)}|$.

Therefore, we have the sparsity coefficients $c_i^{(t)}$ equivalently serving as the status indicator upon convergence, i.e., $c_i^{(t)} = c_H$ corresponds to $\theta_i^{(t)} = 0$ and $c_i^{(t)} = c_L$ corresponds to $\theta_i^{(t)} = 1$. So that the ideal persistency constraint $\theta_i^{(t)} \geq \theta_i^{(t-1)}$ can be transformed into $c_i^{(t)} \leq c_i^{(t-1)}$, and thus embedded into the coefficient toggling process. Algorithm 1 shows the pseudocode of our implementation. After each update on the sparsity coefficients, we solve the sparse optimization problem using the circuit formulation as illustrated in Section II-C, that leverages circuit-inspired optimization heuristics [9] to facilitate fast convergence.

IV. EXPERIMENTS

This Section conducts experiments to evaluate the efficacy of our proposed multi-period method, by answering the following questions:

- 1) **Q1. Persistency:** how persistent are the identified vulnerability locations from our proposed method compared to the baseline method [12]?
- 2) **Q2. Sparsity & total compensations** do we sacrifice sparsity and total compensations while enforcing persistency?
- 3) **Q3. Scalability:** how does our algorithm scale with the system size?

We test and compare two methods:

Algorithm 1: Sparse optimization with persistency prior for scenario t

Input: Prior sparsity coefficients $c^{(t-1)}$; case data $g(\cdot)$ for scenario t
Output: $c_i^{(t)}, n_i^{(t)}, v^{(t)}$

1 **Initialize:** $c_i^{(t)} = c_H$ for \forall location i
2 **Initialize** $n^{(t)}$ by Problem 1 dense optimization.
3 **repeat**
4 Update $c^{(t)}$ from $n^{(t)}$ to set a sparser goal (algorithm in [12]);
5 **Encourage persistency** $c^{(t)} \preceq c^{(t-1)}$:
 $c_i^{(t)} \leftarrow 0.5 \cdot c_L$, for $\forall i$ with $c_i^{(t-1)} \leq c_L$
6 Solve sparse optimization with updated $c^{(t)}$:
 $\min_{\mathbf{x}, \mathbf{n}} \frac{1}{2} \|\mathbf{n}\|_2^2 + \sum_i c_i^{(t)} |\mathbf{n}_i|$ s.t. $g(\mathbf{v}) + \mathbf{n} = 0$
7 **until** fail to converge to sparser solution;

- **(Proposed) Multi-period method** in Section III
- **(Baseline) Single-scenario method** [12] that solves Problem 2 separately for each scenario

Case data and experiment settings: This paper tests on standard IEEE cases of transmission systems. For each test case, we generate $T = 10$ synthetic collapsed (i.e., blackout) scenarios by increasing the load factor incrementally. Load factor is the scaling factor used to increase the original power load. Notably, although this paper mainly experiments on uniformly growing load factors across the entire grid, the proposed work itself is agnostic to demand patterns, and applies without generality to uneven load growth where some areas grow faster than others.

In Section IV-A, we show results of CASE30 and CASE2383WP [25], evaluating location persistency (Definition 2) and set persistency (Definition 3) of baseline method and proposed multi-period method. In Section IV-B, we compare their sparsity and total compensation. Finally, in Subsection IV-C, test cases of different sizes are used to evaluate run time and scalability. All experiments were conducted on a Microsoft Windows 11 desktop with 3.6 GHz Intel i7-12700K Core and 32 GB RAM.

A. Persistency

We show results on IEEE standard 30-bus case CASE30 with load factors $3.8, 3.9, \dots, 4.7$; and CASE2383WP which is a 2383-bus case representing part of the European high voltage network, using load factors $1.35, 1.36, \dots, 1.44$. Figure 1 provides a graphical illustration of the results.

Figure 3 and Figure 4 show the persistency metrics on CASE30 and CASE2383WP respectively. Results show the proposed method achieve higher location persistency and set persistency than the baseline.

B. Sparsity and total compensation

The key goal of sparse diagnosis is to give targeted and focused insights of key vulnerable locations. In general, higher

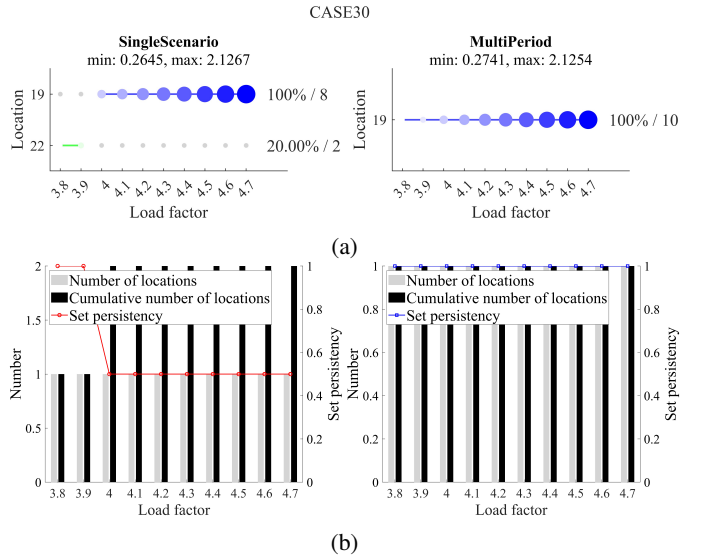


Fig. 3: CASE30 Persistency: single-scenario (left) VS proposed multi-period (right) method. Subfigure (a) lists the key vulnerable locations at each scenario and plot the magnitude of key vulnerability sources $|n_i^{(t)}|$ by the size of the colored circle markers. Our proposed method (right) identifies bus #19 as the only vulnerable location starting from 1st and persists until the last scenario; the location is a 100% persistent failure location, i.e., the location persistency is 100%, and it lasts for 10 steps in total (as notified on the right with “100% / 10”). Whereas the baseline method (left) locates vulnerability sources to bus #22 in 1st and 2nd scenario; and later switched to bus #19, leading to lower persistency. The bottom plots (b) illustrate overall persistency by SetPersistency metric for baseline (left) and proposed (right) method. Bar plots show the number of locations $|\mathcal{S}^{(t)}|$ and the cumulative number of locations $|\sum_{j=1}^t \mathcal{S}^{(j)}|$ for $\forall t$; and red/blue line plot shows the ratio between the two, which is $\text{SetPersistency}(t) = |\mathcal{S}^{(t)}| / |\sum_{j=1}^t \mathcal{S}^{(j)}|$ for $\forall t$.

sparsity is more desirable. So we evaluate whether the proposed method leads to less sparse solutions (i.e., more vulnerabilities) than the baseline, while encouraging persistency.

Meanwhile, the total amount of vulnerability sources represents intuitively the overall severity of the collapse and the total necessary compensation resources needed to restore system feasibility. Therefore, we evaluate whether the proposed method leads to a larger amount of total compensation resources, which could increase the risk of exaggerating severity or “wasting” resources.

Figure 5 shows the results on CASE2383WP. Figure 5a compares the sparsity, i.e. $|\mathcal{S}^{(t)}|$, of two methods, and shows that two methods are comparable, meaning that our proposed method does not significantly sacrifice sparsity when seeking to achieve the expected persistency. Figure 5b also shows that the total compensation is not sacrificed.

Furthermore, from a practical perspective, a sparser solution together with a smaller total compensation generally means

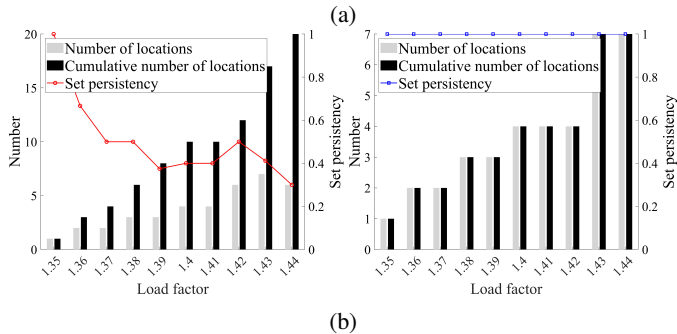
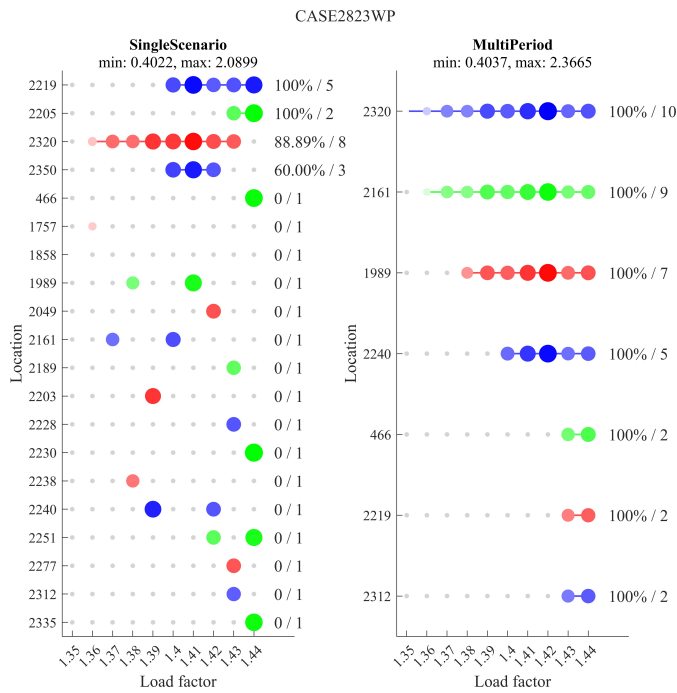


Fig. 4: CASE2383WP Persistence: single-scenario (left) VS proposed multi-period (right) method. (a): using single-scenario baseline, only 2 persistent vulnerability locations (No. 2219 and 2205) are identified No. 2320 and 2350, all other vulnerable locations do not persist well. Whereas using the proposed method, all identified vulnerability locations are persistent failure sources. (b): set persistency decreases with as we process more scenarios using baseline method; whereas our proposed method maintains high set persistency.

less additional power planning. A major advantage brought by persistency is to minimize intervention not just for a single scenario, but for a time window of multiple scenarios. E.g., when load demand increases at the next stage, it can be handled by slightly modifying the plan decision of the previous stage (e.g., making an already planned power plant bigger), instead of switching to a completely different plan.

C. Scalability

To verify the scalability of our proposed method, we evaluate the run time of different sized systems. With similar experiment settings as above, we tested in collapsed scenarios 10 for each system by incrementally increasing

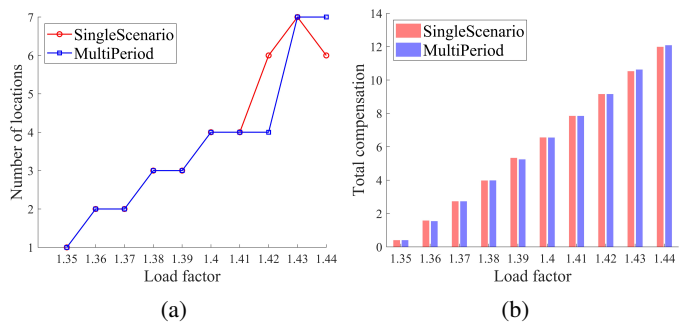


Fig. 5: CASE2383WP: Proposed multi-period method and the single-scenario baseline achieve comparable level of sparsity (left) and total amount of compensation sources (right) to restore feasibility. I.e., our proposed work promotes persistency on multiple scenario analysis without significantly sacrificing sparsity and compensation resources.

their load factors within a range: CASE30[25] (load factor: 3.8~4.8), CASE118[25] (load factor: 3.5~4.5), CASE300[25] (load factor 1.05~1.1), CASE1354PEGASE[26][27] (load factor 1.32~1.35), CASE2383WP[25] (load factor 1.35~1.45), and CASE3375WP (load factor 1.2~1.3). Result in Figure 6 shows that our proposed method scales well on large-scale systems; and with run time being comparable with the single-scenario baseline. This verifies that our multi-period approach encourages persistency in an efficient way without introducing significant computation burden. Moreover, it is worth noting that analyzing power flows under various load growth scenarios (the use case being considered here) is primarily a system planning application. In this context, the capability to solve for systems with thousands of buses in just 3-4 minutes (200 seconds) is highly promising and shows the computational robustness of the proposed methodology.

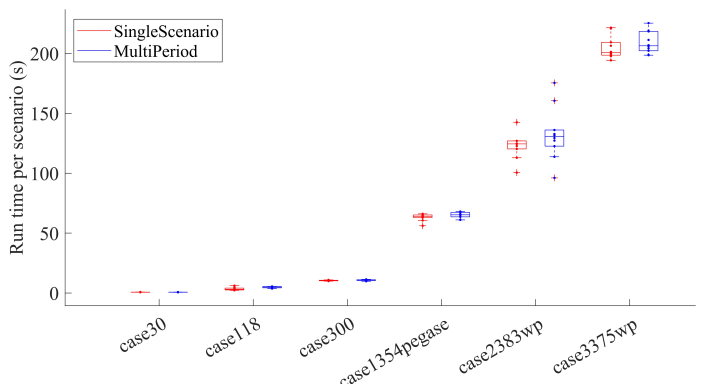


Fig. 6: Comparison of per-scenario run time. Each scatter point represents the run time for a scenario in the test case, and correspondingly the box plot describes the summary statistics, including median, 25th and 75th percentiles, minimum and maximum values.

V. CONCLUSION

This paper proposes a novel multi-period sparse optimization to identify the vulnerable locations responsible for multiple power system blackouts induced by extremely high demand conditions. Compared with analyzing each single scenario separately, our multi-period method sorted all scenarios in the order of growing stress to form a sequence of multi-period practical load-growth scenarios; and then encouraged persistency in vulnerability identification problem while solving for these cases. We defined the ideal persistency of vulnerability sources, and two evaluation metrics: locational persistency and set persistency. Experiments on benchmark systems show that the method 1) reliably tracks persistent failure locations under increasing load stress, pinpointing 7 persistent vulnerability locations on CASE2383WP with the range of 35%~44% load increase; 2) and solves with scalability to large systems (taking < 4min on 3000+ bus systems). Moreover, by capturing inherent vulnerabilities across a continuous stress spectrum, this work enables projections to intermediate load-growth scenarios not explicitly solved. In planning studies, this capability reduces the need to evaluate every critical case individually, thereby significantly improving efficiency. And although this paper mainly experiments on uniformly growing load factors across the entire grid, the proposed work itself is agnostic to demand patterns, and applies without generality to uneven load growth where some areas grow faster than others.

REFERENCES

- [1] B. Singer, A. Pandey, S. Li, L. Bauer, C. Miller, L. Pileggi, and V. Sekar, “Shedding light on inconsistencies in grid cybersecurity: Disconnects and recommendations,” in *2023 IEEE Symposium on Security and Privacy (SP)*. IEEE Computer Society, 2023, pp. 554–571.
- [2] J. W. Busby, K. Baker, M. D. Bazilian, A. Q. Gilbert, E. Grubert, V. Rai, J. D. Rhodes, S. Shidore, C. A. Smith, and M. E. Webber, “Cascading risks: Understanding the 2021 winter blackout in texas,” *Energy Research & Social Science*, vol. 77, p. 102106, 2021.
- [3] D. U. Case, “Analysis of the cyber attack on the ukrainian power grid,” *Electricity Information Sharing and Analysis Center (E-ISAC)*, vol. 388, 2016.
- [4] R. M. Lee, M. Assante, and T. Conway, “Crashoverride: Analysis of the threat to electric grid operations,” *Dragos Inc., March*, 2017.
- [5] S. Soltan, P. Mittal, and H. V. Poor, “{BlackIoT}:{IoT} botnet of high wattage devices can disrupt the power grid,” in *27th USENIX security symposium (USENIX security 18)*, 2018, pp. 15–32.
- [6] S. Li, A. Pandey, and L. Pileggi, “Contingency analysis with warm starter using probabilistic graphical model,” *Electric Power Systems Research*, vol. 234, p. 110737, 2024.
- [7] P. Pourbeik, P. S. Kundur, and C. W. Taylor, “The anatomy of a power grid blackout-root causes and dynamics of recent major blackouts,” *IEEE Power and Energy Magazine*, vol. 4, no. 5, pp. 22–29, 2006.
- [8] V. Ajjarapu and C. Christy, “The continuation power flow: a tool for steady state voltage stability analysis,” *IEEE transactions on Power Systems*, vol. 7, no. 1, pp. 416–423, 1992.
- [9] M. Jereminov, D. M. Bromberg, A. Pandey, M. R. Wagner, and L. Pileggi, “Evaluating feasibility within power flow,” *IEEE Transactions on Smart Grid*, vol. 11, no. 4, pp. 3522–3534, 2020.
- [10] A. Pandey, M. Jereminov, M. R. Wagner, D. M. Bromberg, G. Hug, and L. Pileggi, “Robust power flow and three-phase power flow analyses,” *IEEE Transactions on Power Systems*, vol. 34, no. 1, pp. 616–626, 2018.
- [11] T. J. Overbye, “A power flow measure for unsolvable cases,” *IEEE Transactions on Power Systems*, vol. 9, no. 3, pp. 1359–1365, 1994.
- [12] S. Li, A. Pandey, A. Agarwal, M. Jereminov, and L. Pileggi, “A lasso-inspired approach for localizing power system infeasibility,” in *2020 IEEE Power & Energy Society General Meeting (PESGM)*. IEEE, 2020, pp. 1–5.
- [13] E. Foster, A. Pandey, and L. Pileggi, “Three-phase infeasibility analysis for distribution grid studies,” *Electric Power Systems Research*, vol. 212, p. 108486, 2022.
- [14] M. H. Ali and A. Pandey, “Distributed primal-dual interior point framework for analyzing infeasible combined transmission and distribution grid networks,” *arXiv preprint arXiv:2409.14532*, 2024.
- [15] M. Mandala and C. P. Gupta, “Congestion management by optimal placement of facts device,” in *2010 Joint International Conference on Power Electronics, Drives and Energy Systems & 2010 Power India*. IEEE, 2010.
- [16] M. M. Farsangi, H. Nezamabadi-pour, Y. H. Song, and K. Y. Lee, “Placement of svcs and selection of stabilizing signals in power systems,” *IEEE Transactions on Power Systems*, vol. 22, no. 3, pp. 1061–1071, 2007.
- [17] N. K. Sharma, A. Ghosh, and R. K. Varma, “A novel placement strategy for facts controllers,” *IEEE Transactions on Power Delivery*, vol. 18, no. 3, pp. 982–987, 2003.
- [18] R. Benabid, M. Boudour, and M. A. Abido, “Optimal location and setting of svc and tsc devices using non-dominated sorting particle swarm optimization,” *Electric Power Systems Research*, vol. 79, no. 12, pp. 1668–1677, 2009.
- [19] P. W. Tuinenga, *SPICE: a guide to circuit simulation and analysis using PSpice*. Prentice Hall, 1995, vol. 2.
- [20] S. Li, A. Pandey, S. Kar, and L. Pileggi, “A circuit-theoretic approach to state estimation,” in *2020 IEEE PES Innovative Smart Grid Technologies Europe (ISGT-Europe)*, 2020, pp. 1126–1130.
- [21] S. Li, A. Pandey, and L. Pileggi, “A wlav-based robust hybrid state estimation using circuit-theoretic approach,” *arXiv preprint arXiv:2011.06021*, 2020.
- [22] A. Pandey, S. Li, and L. Pileggi, “Combined transmission and distribution state-estimation for future electric grids,” in *Power Systems Operation with 100% Renewable Energy Sources*. Elsevier, 2024, pp. 299–315.
- [23] S. Li, A. Pandey, and L. Pileggi, “A convex method of generalized state estimation using circuit-theoretic node-breaker model,” *arXiv preprint arXiv:2109.14742*, 2021.
- [24] M. Jereminov, A. Pandey, and L. Pileggi, “Equivalent circuit formulation for solving ac optimal power flow,” *IEEE Transactions on Power Systems*, vol. 34, no. 3, pp. 2354–2365, 2018.
- [25] R. D. Zimmerman, C. E. Murillo-Sánchez, and R. J. Thomas, “Matpower: Steady-state operations, planning, and analysis tools for power systems research and education,” *IEEE Transactions on power systems*, vol. 26, no. 1, pp. 12–19, 2010.
- [26] C. Josz, S. Fliscounakis, J. Maeght, and P. Panciatici, “Ac power flow data in matpower and qcqp format: itesla, rte snapshots, and pegaso,” *arXiv preprint arXiv:1603.01533*, 2016.
- [27] S. Fliscounakis, P. Panciatici, F. Capitanescu, and L. Wehenkel, “Contingency ranking with respect to overloads in very large power systems taking into account uncertainty, preventive, and corrective actions,” *IEEE Transactions on Power Systems*, vol. 28, no. 4, pp. 4909–4917, 2013.